Improving Droplet Microfluidic Systems for Studying Single Bacteria Growth

Yesman Akuoko, Heitor F. Nagliati, Calton J. Millward, Adam T. Woolley*

Department of Chemistry and Biochemistry, Brigham Young University, Provo, UT 84602, USA

*Corresponding Author: phone 1-801-422-1701; atw@byu.edu.

Abstract

Antimicrobial resistance remains a global threat with ~5 million deaths in 2019 alone and 10 million deaths projected every year by 2050. Current tools employed in the analysis of bacteria can be time inefficient, leading to delayed diagnosis and treatment. In this work, we develop a microfluidic setup capable of bacteria incubation and detection of growth in ~2 h. We fabricated polydimethylsiloxane (PDMS) microchips via soft lithography, enclosed microchannels by plasma bonding to glass, and utilized PDMS blocks for simplified connection of devices to a flow system. We generated uniform droplets enclosing zero, one or two bacteria within our devices, and incubated droplet-encapsulated bacteria with 100× lower concentrations of a fluorescence probe of bacterial growth compared to prior work. We assessed bacterial growth via laser induced fluorescence after room temperature incubation for 2 h and obtained a range of signals corresponding to droplets with or without bacteria. Our devices allow for online droplet incubation, monitoring, detection, and tracking. Developing microfluidic chips for single bacteria studies will improve the analysis and treatment of antimicrobial resistance.

Keywords

Single bacteria analysis, Antimicrobial susceptibility testing, Resazurin, Polydimethylsiloxane, Microfabrication

Introduction

Antimicrobial resistance remains a global threat with ~5 million deaths in 2019 alone and 10 million deaths projected every year by 2050 [1]. In the US, the Centers for Disease Control and Prevention reported ~2.8 million antimicrobial resistant infections and 35,000 deaths occurring annually [2]. Current tools employed in the diagnosis of antimicrobial resistance can be time inefficient leading to delayed diagnosis and treatment [3,4]. New techniques for improved study of bacteria will reduce mortality rate, antimicrobial resistance and medical costs resulting from delayed treatment [5,6].

Microfluidics as a platform for novel analytical tools has been explored for some time [5,7-16]. Microfluidic applications include DNA analysis [5,8,11,13,16], bacterial analysis [7,9,14] and single-cell genomics [10,15] to name a few. Droplet microfluidic systems use immiscible phases to confine contents in discrete droplets [17,18], which can be advantageous for controlling diffusional losses, high-throughput biological experiments or automated control of multiple microreactors. Bacteria can be grown within discrete droplets and when enclosed with appropriate reagents, online analysis can be performed [19]. This type of single-cell analysis helps overcome limitations associated with ensemble-averaged data from multiple cells [18].

Various droplet microfluidic setups or techniques for examining bacteria growth have been reported. Boedicker et al. [20] presented a method for performing susceptibility testing of bacteria which involved trapping bacteria cells in nL-sized plugs for incubation, imaging and fluorescence detection. Plugs enclosing *S. aureus* bacteria were collected in Teflon tubing and analyzed for >7 h in a microscope incubator; however, the setup employed off-chip incubation and long assay times. Keays et al. [21] also utilized a tubing system for droplet generation, incubation, and monitoring of bacterial cell growth. The setup utilized a plate reader to record changes in optical

density of droplets to determine the growth rate of encapsulated bacteria over 10 h. A droplet microfluidic system with an array of docking sites capable of trapping individual droplets was developed by Kang et al. [22]. The microfluidic platform comprised four units each with >8000 droplet docking sites, and each docking station could trap droplets containing 1-4 bacteria cells and be monitored over 2 h duration. Kaushik et al. [9] developed droplet-based microfluidic chips for studying the growth of single bacteria in pL-sized droplets in a shorter time. The confinement of bacteria in small droplet incubation chambers coupled with resazurin-based fluorescence detection provided assay results in ~1 h.

The above-mentioned works demonstrate capability for droplet microfluidics of bacteria; however, these techniques either lose droplet traceability, require high levels of fluorescence reporter molecules, lack single cell studies, or require offline incubation and monitoring. Notably, droplet destabilization and unwanted merging can occur during the transfer of droplets with offline systems [23], particularly limiting droplet traceability.

Herein, we develop a microfluidic setup capable of studying single bacteria growth in droplets over 2 h. We use PDMS blocks as microfluidic tubing connectors to simplify interfacing with flow systems. Our devices allow for online incubation, droplet monitoring and detection, offering an integrated setup with potential for future automation and rapid availability of assay results. We performed bacteria counts in droplets with microscopic imaging and demonstrated the encapsulation of single bacteria with our droplet microfluidic platform. We studied droplet-encapsulated *E. coli* in our devices and evaluated room temperature growth over multiple hours. Even with a 100× lower concentration of fluorescent probe compared to earlier studies we were able to confirm bacteria viability. We use this platform to monitor the growth of single *E. coli* cells

over 2 h in room temperature incubation conditions. Our setup's ability to avoid droplet overlap or desequencing will enable droplet tracking in future studies.

Materials and methods

Chemicals and materials

The following materials were used in making the PDMS-glass microfluidic devices: Sylgard 184 silicone elastomer base and curing agent (H047LAC000, Midland, MI), glass slides (1 mm thick, 12-550C, Thermo Fisher Scientific, Waltham, MA), cover glass (0.13-0.16 mm thick, 5075-1D, Thermo Fisher Scientific) and Aquapel (47112, Cranberry, PA). The SU-8 2075 photoresist used in photolithography was obtained from Kayaku Advanced Materials (Westborough, MA). The continuous phase for the water-in oil (W/O) droplets was composed of Novec 7500 engineered fluid and polytetrafluoroethylene-polyethylene glycol-polytetrafluoroethylene (PTFE-PEG-PTFE) surfactant purchased from 3M (St. Paul, MN) and Creative PEGWorks (Chapel Hill, NC), respectively. The bacteria gram staining kit, the lysogeny broth and agar media (Difco brand) were obtained from Thermo Fisher Scientific. All broth solutions and deionized water (18.3 MΩ) were autoclaved before use. The *Escherichia coli* (ATCC 29522) bacterial strain and resazurin sodium salt (AAB2118706) were procured from ATCC and Thermo Fisher Scientific, respectively.

Device design and fabrication

Microfluidic channels of dimensions 200 × 75 μm^2 (width by height) were designed using CleWin software, and PDMS microfluidic devices were fabricated from molds created using standard photolithography. In brief, the chrome mask design was patterned onto a 4 in. Si wafer coated with SU-8 2075 photoresist. When the Si-wafer molds were ready, PDMS mixture from combining

Sylgard 184 base to curing agent at a 10:1 ratio was poured onto the Si wafer and baked at 70 °C for ~20 min. The PDMS replicas were then bonded to glass slides via oxygen plasma treatment in a plasma cleaner (PDC-32G, Harrick Plasma). Cube-shaped PDMS blocks ($0.5 \times 0.5 \times 0.5$ cm^3) were used as microfluidic connectors for attachment of PTFE tubing to the microfluidic devices. The connectors were perforated with a 1.5 mm biopsy punch (Integra Life Sciences, Mansfield, MA) and attached to the PDMS-glass devices using freshly degassed PDMS. The microfluidic devices were then left to bake in an oven at ~80 °C for 30 min, and the microchannels were later treated with Aquapel, flushed with nitrogen, and baked at ~80 °C for 30 min.

Device and experimental operation

Droplet generation and fluorescence measurements were achieved using the fluid control and detection system described in prior work with slight modifications [5]. The Fluigent pump system (Le Kremlin-Bicêtre, France) was used for fluid control and generation of W/O droplets. A pump system pressure of 500 mbar was used for both oil and sample aqueous phases. The optical setup for fluorescence measurements consisted of a solid-state 532 nm laser (CrystaLaser, Reno, NV), optical filters, a photomultiplier, and a data display LabVIEW (National Instruments, Austin, TX) program as described previously [24]. For W/O droplet generation, the oil phase was mixed with 0.1 % (w/w) PTFE-PEG-PTFE surfactant, and the sample aqueous phase consisted of LB media, 500 nM resazurin and 2×10^8 CFU/mL *E. coli*. We used 0.1% (w/w) surfactant in oil to avoid micelle formation and material transport between droplets, and to minimize droplet shrinkage [25,26]. After droplets were generated in-chip, the initial fluorescence signal was measured in the optical setup, and the droplet-encapsulated bacteria were incubated in-chip at room temperature for ~2 h, after which the fluorescence signal from incubated droplets was measured again.

Bacteria staining, imaging, and cell counting

To demonstrate the ability of our setup to encapsulate single bacteria in W/O droplets, 2×10^8 CFU/mL of *E. coli* was initially centrifuged, and the solid residue mixed with both crystal violet and Gram's iodine before decolorization with acetone, and then counterstained with safranin dye. Each staining step was performed in between rinse, centrifugation, and decanting steps. The final solution was centrifuged, and the solid residue made up of labeled *E. coli* cells was diluted with LB media and used as the aqueous phase in generating W/O droplets. Droplets were generated in microfluidic channels with dimensions of 100×10 μm^2 (width by height) and visualized with a 100× Nikon Plan Fluorite oil immersion objective (Melville, NY) and a CCD camera (C14440-C0UP, Hamamatsu, Japan). For bacteria imaging, thinner (0.13-0.16 mm) cover glass slides were used in fabricating the PDMS-glass microfluidic devices.

Results and discussion

Device setup and operation

Figure 1a shows the microchannel design with oil and aqueous inlets for droplet generation, a mixing zone for complete blending of droplet components, and an incubation zone for storing of droplets for ~2 h before fluorescence detection. The detection point is located near the outlet of the microchannel, although the device setup and operation also allow detection to be accomplished anywhere in the incubation zone. Figure 1b displays a top view photograph of a completed PDMS microfluidic device filled with red food dye solution for easy visualization of the microchannel, and Figure 1c shows uniform-sized W/O droplets generated in a microchannel, enroute to the incubation zone. PDMS microfluidic devices often are created as thick layers to allow microfluidic connector tubing to be held in place by the PDMS device material [9,22]. As an alternative, we utilized cube shaped PDMS blocks for attachment of PTFE tubing to the microfluidic devices, so the final microfluidic devices were more compact and required less PDMS (see ESM Fig. S1).

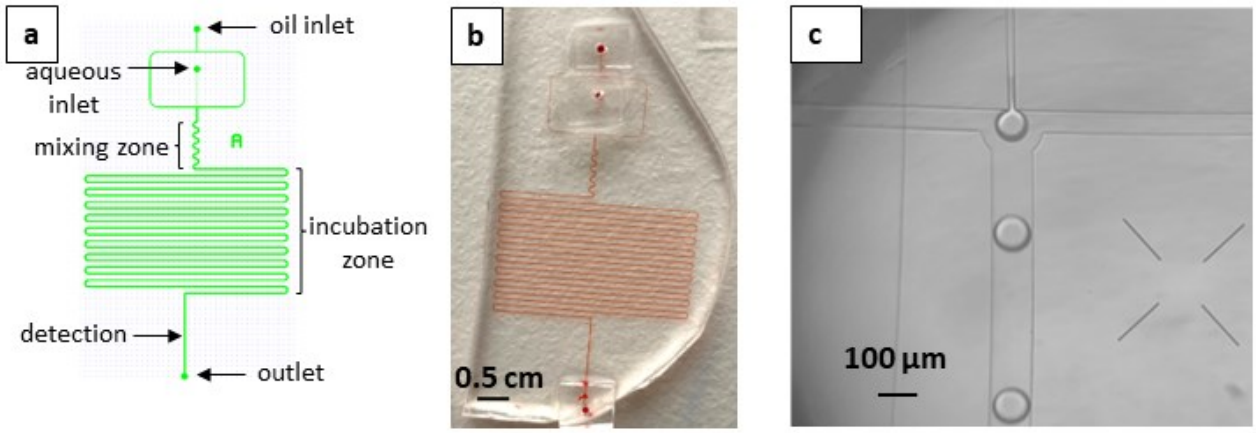

Fig. 1 *Microdevices for droplet microfluidics. (a) Schematic view of PDMS microdevice. (b) Top-view photograph of PDMS microdevice. (c) W/O droplet generation in microchannel.*

We studied various microchannel depths ranging from 10 to 200 µm and widths from 10 to 100 µm. W/O droplets generated in shallower or narrower microchannels lost volume during incubation. Channel depths below 75 µm produced rod-shaped droplets, which fully contacted the PDMS microchannel walls, potentially leading to analyte or solvent transport to the bulk PDMS [27]. On the basis of these data, we used microchannel dimensions of 200 × 75 μm^2 (width by height). We utilized a Fluigent flow control system (see ESM Fig S1b), which provided constant pressure-driven flow rates and reproducible W/O droplet volumes. The final setup provided steady generation of 40–70 droplets/min with uniform sizes as seen in Fig. 1c and ESM Movie S1. The mean (± standard deviation) droplet diameter was 155 ± 15 µm, corresponding to a calculated volume of 1.7 ± 0.4 nL [28].

Bacteria cell count and fluorescence measurements

In Figure 2, we show the ability of our setup to generate droplets that contain single bacteria. Figure 2a-b shows droplets containing single bacteria (circled in red), while Figure 2c-d shows droplets containing two bacteria each. Controlling the droplet size via aqueous and oil phase flow

rates, and selecting the concentration of bacteria solution allowed droplets with desired numbers of bacteria to be made. Figure 3 shows a histogram of the number of droplets containing zero, one or two bacteria. About 60% of the droplets imaged under these conditions had no bacteria, while ~33% had single bacteria and ~7% had two bacteria, which is consistent with Poisson distribution statistics [29].

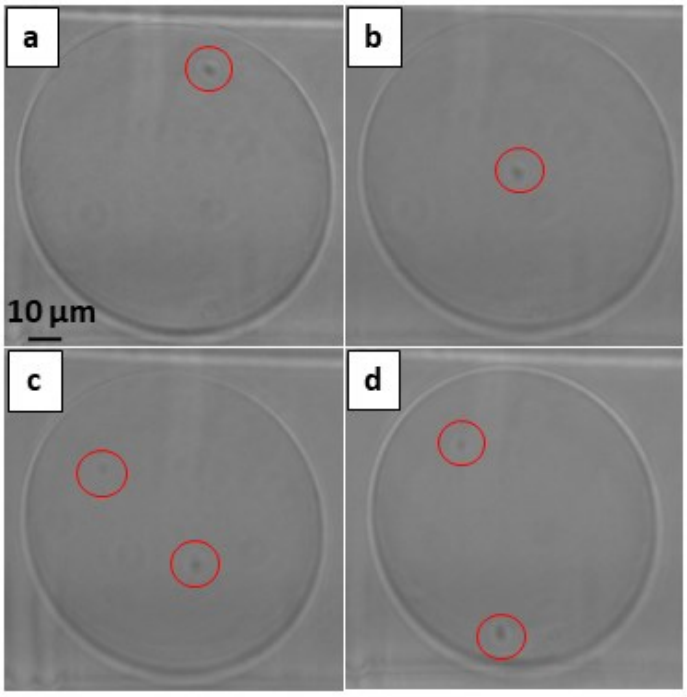

Fig. 2 *Images of W/O droplets containing E. coli. (a-b) Single bacteria in a droplet and (c-d) two bacteria in a droplet.*

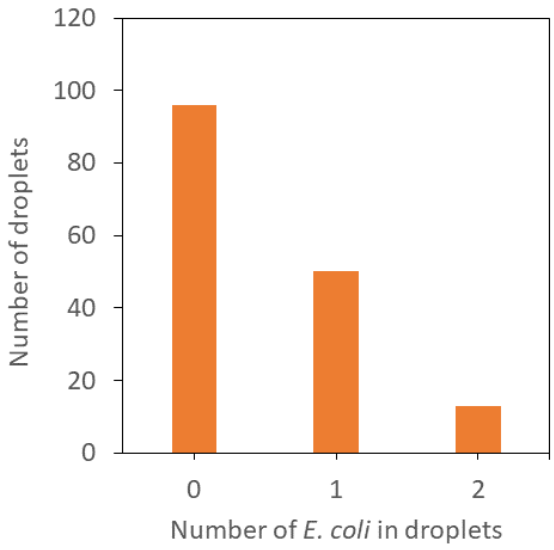

Fig. 3 *Distribution of E. coli in W/O droplets (n = 159).*

E. coli is a robust microorganism capable of replicating over a wide range of temperatures and growth conditions. *E. coli* replicates approximately every 20 min under optimal aerobic conditions in LB broth at pH 7.0 and 37 °C. We performed our experiments in the same solution but at room temperature. Growing and dividing *E. coli* produce NADH, which reduces non-fluorescent resazurin to fluorescent resorufin, resulting in an increase in fluorescent signal. We evaluated *E. coli* droplet incubation times ranging from 1-5 h in our detection setup. Before/after fluorescence signal differences were difficult to discern after 1-h incubation. The fluorescence signal often exceeded the dynamic range of our detection setup after incubation times >3 h. We thus selected 2 h incubation times for experiments as a compromise between signal and experimental time. Other droplet microfluidic studies reported in the literature on bacteria with resazurin utilized >50 µM resazurin concentrations [9,20]. Utilizing µM resazurin concentration potentially causes any slight amounts of resorufin produced from bacteria growth to dilute into the bulk resazurin, further increasing incubation times. We utilized a 100× lower concentration of resazurin for our

experiments, which reduced background and allowed slight changes in resorufin concentration during incubation to be picked up in fluorescence detection.

To demonstrate successful bacteria incubation within droplets, we studied droplets generated from a sample solution containing 2×10^8 CFU/mL *E. coli*, 500 nM resazurin and LB broth. The use of low concentrations of fluorescent label reduces costs and waste, limits perturbation to bacteria and allows low resorufin concentrations produced post incubation to be effectively detected, potentially limiting false positive results. High concentrations of resazurin have further been reported to limit cell survivability over extended incubation times [30], so our approach is well-suited for applications requiring extended incubation of cells with resazurin. Figure 4 shows the fluorescence vs. time profile from streams of droplet-encapsulated bacteria before and after incubation. We observe RFU signals with similar peak heights from droplets before incubation as seen in Fig. 4a. In contrast, in Fig. 4b we observe RFU signals with varying peak heights after incubation. We show an expanded view of the data from Fig. 4a and 4b in Fig. 4c and 4d. The RFU signal from each droplet before incubation was 2.7 ± 0.02 RFU ($n = 243$) in Fig. 4a. After 2 h incubation, peaks in Fig. 4b range from 1.5–6.5 RFU. The increase in RFU in some droplets is supportive of the presence of one or more bacteria and their growth in the droplets during the incubation period. Droplets with static or decreased fluorescence after 2 h incubation likely lack encapsulated bacteria; a decrease in RFU for some droplets after incubation could be from loss of analyte from droplet(s) during that time. Changes in droplet spacing in the fluorescence data before and after incubation (Fig. 4) occur when droplets undergo relative motion, creating clusters with reduced space in between. Slight backpressure during flow of droplets through the incubation zone may also lead to minor compression in the droplet spacing observed.

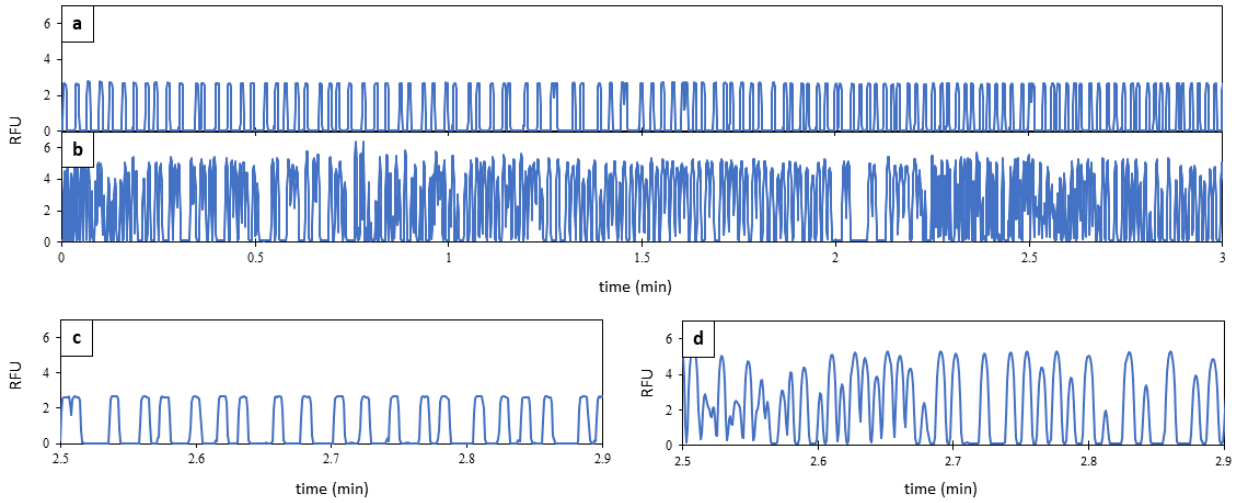

Fig. 4 *LIF of droplets containing 2 × 10^8 CFU/mL E. coli and LB broth. (a) Before incubation and (b) after ~2 h incubation. (c) Zoomed view of data in (a). (d) Zoomed view of data in (b).*

To confirm that the fluorescence increase in Fig. 4 is due to droplet-encapsulated bacteria, we performed control experiments involving droplets without bacteria. The fluorescence-time profile in ESM Fig. S2a-b clearly shows that the droplet fluorescence before and after incubation is largely unchanged. These data confirm a lack of resorufin production during incubation due to the absence of bacteria in droplets. Small changes in fluorescence signal are attributed to minor droplet shrinkage or generation of small amounts of resorufin from resazurin reduction under the incubation conditions, and similar outcomes were obtained in replicate experiments. Changes in spacing between peaks before and after incubation (see Fig. 4b and ESM Fig. S2b) could be attributed to relative motion between droplets during incubation (see ESM Fig. S3), also resulting in altered spacing and closer proximity between some adjacent droplets producing fluorescence signals which are not baseline resolved in Fig. 4 and ESM Fig. S2.

To further demonstrate the changes in fluorescence in bacteria-encapsulated droplets after on-chip incubation, we generated histograms of droplet fluorescence. In Fig. 5a and 5b, we provide histogram distributions showing the fluorescence signal of droplets for a control experiment. Fig. 5a shows a single peak (1.25 ± 0.03 RFU, n = 213) before incubation, with no change after incubation in Fig. 5b (1.25 ± 0.03 RFU, n = 196). This is further supported by the expanded view images where we observe no change in peak heights for RFU signals before incubation (Fig. S2c) and after incubation (Fig. S2d). In contrast, the histograms in Fig. 5c and 5d show the RFU signal of *E. coli* containing droplets before and after incubation. Fig. 5c shows a single peak (2.7 ± 0.02 RFU, n = 243) before incubation and multiple peaks after incubation (Fig. 5d) demonstrating the presence and growth of *E. coli* in some droplets, with some droplets likely enclosing different numbers of bacteria. The higher pre-incubation droplet fluorescence signal in Fig. 4c relative to Fig. S2c is likely due to between-day variations in optical system alignment. Our incubation channel is designed to retain droplet ordering, which could enable droplet tracking before and after incubation in future studies. As further evidence of this possibility, we demonstrated droplet tracking within our devices by generating different sequences of colored dye (red and green) W/O droplets and tracked them from the incubation region to the outlet/detection region. Fig. S4 in the ESM shows that droplets maintain their sequence and avoid mixing/merging between incubation and detection, further demonstrating potential for tracking.

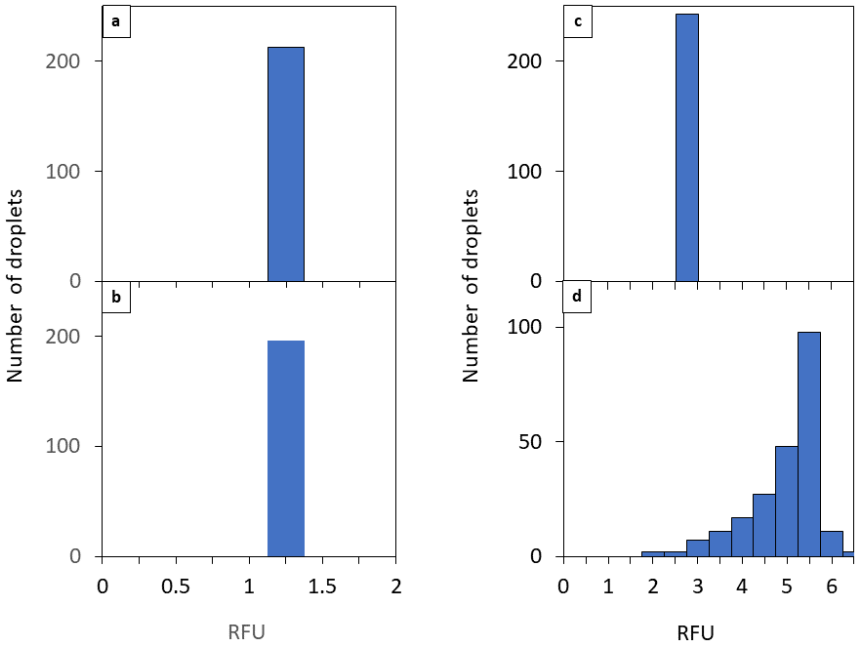

Fig. 5 *Histograms of RFU signals. (a) Bacteria-free droplets before incubation and (b) after ~2 h incubation. (c) Droplets containing 2 × 10^8 CFU/mL E. coli (c) before incubation and (d) after ~2 h incubation. Bin width is 0.5 RFU.*

Conclusions

In summary, we demonstrated an approach to making compact PDMS chips with straightforward tubing connections to fluid pump systems for droplet generation, in-chip incubation, and detection of *E. coli* bacteria. We utilized soft lithography and plasma bonding in fabricating our microfluidic devices, and prepared connectors using PDMS blocks for interfacing of our devices to a flow control system. We produced uniform droplets enclosing zero, one or two bacteria within our devices, incubated droplet-encapsulated bacteria with nM concentrations of a fluorescence reporter and performed detection via laser induced fluorescence after convenient room temperature 2h incubation conditions. Our devices allow for online droplet incubation, monitoring, detection, and

traceability all within a single microfluidic device. This platform should allow the testing of various concentrations of antibiotic(s) on single bacteria and could be adapted to work at 37°C in future experiments. Developing microfluidic chips with sample droplet generation and fluorescence detection would advance commercialization and potential field deployment of droplet microfluidic devices for bacteria studies.

Acknowledgements

This research was supported in part by the U.S. National Institutes of Health under grant R01 AI116989 and by a National Science Foundation Research Experience for Undergraduates Grant (CHE-2050872), Brigham Young University's Department of Chemistry and Biochemistry, and Brigham Young University's Integrated Microfabrication Lab.

Declarations

Funding: This research was funded by the U.S. National Institutes of Health (grant R01 AI116989), NSF-REU (grant CHE-2050872), and Brigham Young University.

Conflicts of interest/Competing interests: ATW is chair editor for Analytical and Bioanalytical Chemistry, but was not involved in the peer review of this manuscript. All other authors have no conflicts to report.

Ethics approval: Not applicable

Consent to participate: Not applicable

Consent for publication: Not applicable

Availability of data and material (data transparency): The data that supports the findings of this study are available from the corresponding author upon reasonable request.

Code availability: Not applicable

Authors' contributions (optional): Not applicable

References

1. Antimicrobial Resistance Collaborators. Global burden of bacterial antimicrobial resistance in 2019: a systematic analysis. Lancet. 2022;399:629-55. https://doi.org/10.1016/S0140-6736(21)02724-0
2. Centers for Disease Control and Prevention, Antibiotic Resistance Threats In The United States, 2019.
3. Benkova M, Soukup O, Marek J. Antimicrobial susceptibility testing: currently used methods and devices and the near future in clinical practice. J Appl Microbiol. 2020; 129:806-22. https://doi.org/10.1111/jam.14704
4. Opota O, Croxatto A, Prod'hom G, Greub G. Blood culture-based diagnosis of bacteraemia: state of the art. Clin Microbiol Infect. 2015; 21:313-22. https://doi.org/10.1016/j.cmi.2015.01.003
5. Akuoko Y, Hanson RL, Harris DH, Nielsen JB, Lazalde E, Woolley AT. Rapid and simple pressure-sensitive adhesive microdevice fabrication for sequence-specific capture and fluorescence detection of sepsis-related bacterial plasmid gene sequences. Anal Bioanal Chem. 2021;413:1017-25. https://doi.org/10.1007/s00216-020-03060-2
6. Avesar J, Rosenfeld D, Truman-Rosentsvit M, Ben-Arye T, Geffen Y, Bercovici M, Levennberg S. Rapid phenotypic antimicrobial susceptibility testing using nanoliter arrays. Proc Natl Acad Sci USA. 2017; 114:E5787-E5795. https://doi.org/10.1073/pnas.1703736114

7. Cama J, Voliotis M, Metz J, Smith A, Iannucci J, Keyser UF, Tsaneva-Atanasovaab K, Pagliara S. Single-cell microfluidics facilitates the rapid quantification of antibiotic accumulation in Gram-negative bacteria. Lab Chip. 2020;20:2765-75. https://doi.org/10.1039/d0lc00242a
8. Hanson RL, Lazalde E, Knob R, Harris DH, Akuoko Y, Nielsen JB, Woolley AT. Multilabel hybridization probes for sequence-specific detection of sepsis-related drug resistance genes in plasmids. Talanta Open. 2021;3:100034. https://doi.org/10.1016/j.talo.2021.100034
9. Kaushik AM, Hsieh K, Chen L, Shin DJ, Liao JC, Wang TH. Accelerating bacterial growth detection and antimicrobial susceptibility assessment in integrated picoliter droplet platform. Biosens Bioelectron. 2017;97:260-266. https://doi.org/10.1016/j.bios.2017.06.006
10. Matula K, Rivello F, Huck WTS. Single-Cell Analysis Using Droplet Microfluidics. Adv Biosyst. 2020;4:e1900188. https://doi.org/10.1002/adbi.201900188
11. Mi F, Hu C, Wang Y, Wang Li, Peng F, Geng P, Guan M. Recent advancements in microfluidic chip biosensor detection of foodborne pathogenic bacteria: a review. Anal Bioanal Chem. 2022;414:2883-2902. https://doi.org/10.1007/s00216-021-03872-w
12. Mitchell KR, Esene JE, Woolley AT. Advances in multiplex electrical and optical detection of biomarkers using microfluidic devices. Anal Bioanal Chem. 2022;414:167-180. doi:10.1007/s00216-021-03553-8
13. Nielsen JB, Hanson RL, Almughamsi HM, Pang C, Fish TR, Woolley AT. Microfluidics: Innovations in Materials and Their Fabrication and Functionalization. Anal Chem. 2020;92:150-168. http://dx.doi.org/10.1021/acs.analchem.9b04986

14. Postek W. Pacocha N. Garstecki P. Microfluidics for antibiotic susceptibility testing. Lab Chip. 2022. https://doi.org/10.1039/D2LC00394E
15. Smithers JP, Hayes MA. Interfacing microfluidics with information-rich detection systems for cells, bioparticles, and molecules. Anal Bioanal Chem. 2022;414:4575-89. https://doi.org/10.1007/s00216-022-04043-1
16. Tan SJ, Phan H, Gerry BM, Kuhn A, Hong LZ, Ong Y, Poon PSY, Unger MA, Jones RC, Quake SR, Burkholder WF. A microfluidic device for preparing next generation DNA sequencing libraries and for automating other laboratory protocols that require one or more column chromatography steps. PLoS One. 2013;8:e64084. https://doi.org/10.1371/journal.pone.0064084
17. Collins DJ, Neild A, deMello A, Liud AQ, Ai Y. The Poisson distribution and beyond: methods for microfluidic droplet production and single cell encapsulation. Lab Chip. 2015;15:3439-59. https://doi.org/10.1039/C5LC00614G
18. Kaminski TS, Scheler O, Garstecki P. Droplet microfluidics for microbiology: techniques, applications and challenges. Lab Chip. 2016;16:2168-87. https://doi.org/10.1039/C6LC00367B
19. Qin N, Zhao P, Ho EA, Xin G, Ren CL. Microfluidic Technology for Antibacterial Resistance Study and Antibiotic Susceptibility Testing: Review and Perspective. ACS Sens. 2021;6:3-21. doi:10.1021/acssensors.0c02175
20. Boedicker JQ, Li L, Kline TR, Ismagilov RF. Detecting bacteria and determining their susceptibility to antibiotics by stochastic confinement in nanoliter droplets using plug-based microfluidics. Lab Chip. 2008;8:1265-1272. doi:10.1039/b804911d

21. Keays MC, O'Brien M, Hussain A, Kiely PA, Dalton T. Rapid identification of antibiotic resistance using droplet microfluidics. Bioengineered. 2016;7:79-87. doi:10.1080/21655979.2016.1156824
22. Kang W, Sarkar S, Lin ZS, McKenney S, Konry T. Ultrafast Parallelized Microfluidic Platform for Antimicrobial Susceptibility Testing of Gram Positive and Negative Bacteria. Anal Chem. 2019;91:6242-6249. doi:10.1021/acs.analchem.9b00939
23. Hsieh K, Zec HC, Chen L, Kaushik AM, Mach KE, Liao JC, Wang TH. Simple and Precise Counting of Viable Bacteria by Resazurin-Amplified Picoarray Detection. Anal Chem. 2018;90:9449-9456. doi:10.1021/acs.analchem.8b02096
24. Esene JE, Boaks M, Bickham AV, Nordin GP, Woolley AT. 3D printed microfluidic device for automated, pressure-driven, valve-injected microchip electrophoresis of preterm birth biomarkers. Microchimica Acta. 2022;189:204. https://doi.org/10.1007/s00604-022-05303-8
25. Gruner P, Riechers B, Orellana LAC, Brosseau Q, Maesa F, Beneyton T, Pekin D, Bareta JC. Stabilisers for water-in-fluorinated-oil dispersions: Key properties for microfluidic applications. Curr Opin Colloid Interface Sci. 2015;20:183-191. http://dx.doi.org/10.1016/j.cocis.2015.07.005
26. Skhiri Y, Gruner P, Semin B, Brosseau Q, Pekin D, Mazutis L, Goust V, Kleinschmidt F, El Harrak A, Hutchison JB, Mayot E, Bartolo J-F, Griffiths AD, Taly V, Baret J-C. Dynamics of molecular transport by surfactants in emulsions. Soft Matter. 2012;8. doi:10.1039/c2sm25934f
27. Toepke MW, Beebe DJ. PDMS absorption of small molecules and consequences in microfluidic applications. Lab Chip. 2006;6:1484-86. https://doi.org/10.1039/b612140c

28. Scheler O, Makuch K, Debski PR, Horka M, Ruszczak A, Pacocha N, Sozański K, Smolander OP, Postek W, Garstecki P. Dodecylresorufin (C12R) Outperforms Resorufin in Microdroplet Bacterial Assays. ACS Appl Mater Interfaces. 2016;8:11318-25. http://dx.doi.org/10.1021/acsami.6b02360
29. Najah M, Griffiths AD, Ryckelynck M. Teaching Single-Cell Digital Analysis Using Droplet-Based Microfluidics. Anal Chem. 2012;84:1202-1209. https://doi.org/10.1021/ac202645m
30. Richard TP, Karen JLB. Toxic effects of resazurin on cell cultures. Cytotechnology. 2015;67: 13–17. https://doi.org/10.1007/s10616-013-9664-1